Mass Spectrometry in Weakly Ionized Plasmas Using a Gifford-McMahon Cryocooled Superconducting Magnet

doi: 10.1063/1.1517729

Mass spectrometry in weakly ionized plasmas using a Gifford–McMahon cryocooled superconducting magnet

T. Murakami[a)]
Department of Energy Sciences, Interdisciplinary Graduate School of Science and Engineering, Tokyo Institute of Technology, 4259 Nagatsuta, Midori-ku, Yokohama 226-8502, Japan

T. Kaneko, J. Terashima, and R. Hatakeyama
Department of Electronic Engineering, Tohoku University, 05 Aoba Aramaki-aza, Aoba-ku, Sendai 980-8579, Japan

S. Murase
Department of Electrical and Electronics Engineering, Okayama University, 3-1-1 Tsushima-naka, Okayama 700-8530, Japan

S. Shimamoto
Department of Electrical Engineering, Tohoku University, 05 Aoba Aramaki-aza, Aoba-ku, Sendai 980-8579, Japan

(Received 23 April 2002; accepted 9 September 2002)

Direct mass spectrometry has been successfully conducted even at a high argon gas pressure of the order of 10^{-3} Torr, using a Gifford–McMahon cryocooled superconducting magnet with a magnetic flux density as high as 2 T. A numerical model including collisional effects has been proposed to describe the performance of an omegatron. The intensity of ion current and the mass resolution as functions of pressure and magnetic flux density have been obtained experimentally in the case of argon plasma and compared with those calculated numerically. Collisional effects on the omegatron performance were clarified by this comparison. Although the mass resolution deteriorates under the high-pressure condition, it is predominantly improved in proportion to the magnetic flux density. The collisional effects and the magnetic flux density dependence of the mass resolution at high pressure are clearly explained by the present numerical model. © *2002 American Institute of Physics.* [DOI: 10.1063/1.1517729]

I. INTRODUCTION

The omegatron mass spectroscopic analyzer is a device invented to measure the charge-to-mass ratio of ions in a high-vacuum system through the use of cyclotron resonance.[1] In an omegatron, a high-frequency electric field is set up normal to a uniform dc magnetic flux density, and ions are excited at their various cyclotron resonances, $f_{ci} = \omega_{ci}/2\pi = eB/(2\pi m_i)$ (e is charge, B is magnetic flux density, and m_i is ion mass), causing their orbital radii to increase; the current induced when they strike a collector is measured.

The technique of ion cyclotron resonance has been applied to mass spectrometry[1–5] and isotope separation[6–8] with a small fractional mass difference over a long time, and some specific attempts to improve mass resolution have been performed.[9,10] In most research studies, background pressure in an region of analysis was kept low enough to allow a collisionless analysis to be performed[2,4,6] or differential pumping was applied to maintain the pressure of around 10^{-5} Torr in the region of analysis, which is reduced by a factor of 10^2 in comparison with that in a discharge region.[1,3,5] In those studies, the magnetic flux density $\leqslant 10^{-2}$ T was applied to the region of analysis, except in work carried out by Dawson *et al.* where the flux density of ~ 2 T was produced by a superconducting solenoid coil.[6] At the same time, the mass resolution was predicted theoretically using exact orbit calculations of a charged particle for a collisionless case.[1–3,5,6] The experimental and theoretical results have suggested that in order to increase the resolution, active differential pumping of the analyzer housing must be employed because the resolution is considerably reduced at high neutral pressure, and a strong and uniform magnetic flux density is needed in the region of analysis.

Although the neutral gas pressure of the order of mTorr is generally used in the field of plasma processing, little attention has been paid to ion resonance behavior and no mass spectrometry has been demonstrated at the pressure of around 10^{-3} Torr. Furthermore, little work has focused on calculations for describing collisional effects on omegatron performance. Direct mass spectrometry in a plasma production region without any pump-down system has the advantage of enabling us to efficiently analyze ion species and simplify the apparatus.

In the present study, mass spectrometry has been conducted using an omegatron and a Gifford–McMahon (GM) cryocooled superconducting magnet directly in a plasma production region. A high magnetic flux density of up to 2.0 T is applied to the collision-dominated weakly ionized argon plasma, the pressure of which is of the order of mTorr. Fur-

a)Author to whom correspondence should be addressed; electronic mail: murakami@es.titech.ac.jp

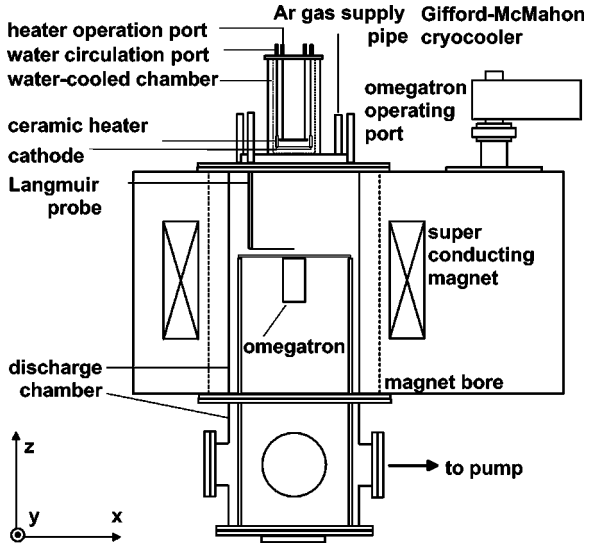

FIG. 1. Schematic configuration of the experimental apparatus consisting of a Gifford–McMahon cryocooled superconducting magnet, an omegatron mass spectroscopic analyzer, an argon gas supply and pumping system, a ceramic heater and cathode as the plasma source, a stainless steel vessel as the discharge chamber, and an electrostatic Langmuir probe measurement system.

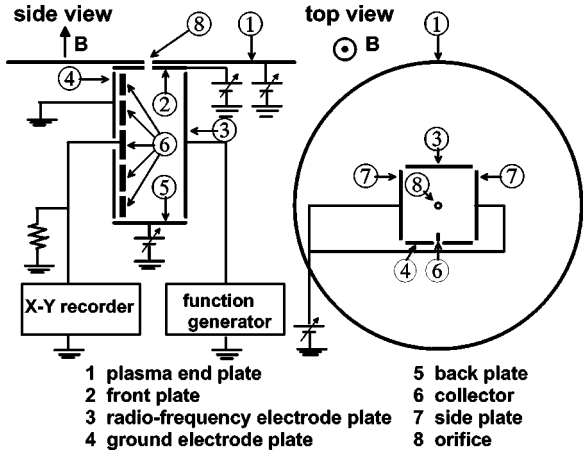

FIG. 2. Schematic side and top views of the omegatron with an electronic circuit for the ion cyclotron resonance mass spectrometer.

thermore, a numerical model including collisional effects has been proposed to describe the performance of the omegatron. First, the mass resolution in the case where ion-neutral particle collisions effect the behavior of ions is examined paying attention to the shapes of ion current spectra. Second, the performance of the omegatron is investigated by varying two operation parameters: the magnetic flux density and argon gas pressure.

II. EXPERIMENTAL PROCEDURE

A. Apparatus

Figure 1 shows a schematic configuration of the experimental apparatus which consists of a GM cryocooled superconducting magnet, an omegatron mass spectroscopic analyzer, an argon gas supply and pumping system, a ceramic heater and barium oxide (BaO) cathode as the plasma source, a stainless steel vessel as the discharge chamber, and an electrostatic Langmuir probe measurement system. The GM cryocooler belongs to a class of cooling systems utilizing a gas-compression refrigeration cycle. The refrigeration effect results from a series of thermodynamic processes acting on the gas, including charging and compression, displacement and heat exchange with a regenerator, and expansion and heat absorption (cooling effect).[11] The superconducting solenoid coil (NbTi) produces a constant magnetic flux density in the axial (z-) direction in the magnet bore of the length of 505 mm and diameter of 400 mm. The magnetic flux-density strength on the axis center of the bore B_{center} is $\leqslant 2.0$ T and inhomogeneity $\Delta B/B_{\text{center}}$ is less than 1% in the omegatron region.

The discharge chamber with a length of 900 mm and inner diameter of 305 mm is immersed in the magnet bore. Argon gas is introduced into the discharge chamber made of stainless steel through a pipe, and exhausted to a diffusion pump through a downstream vessel. The pressure in the regions of discharge and analysis is controlled in the range of $1.0\times10^{-4}\sim1.0\times10^{-3}$ Torr. Since the flow rate is quite low, the flow velocity can be negligible and the argon gas pressure is considered to be constant. Argon ions are produced in the upstream region of the vacuum chamber by direct-current (dc) discharge with a hot BaO cathode, which is heated by a pyrolytic graphite–pyrolytic boron nitride ceramic heater at over 1100 °C. The ions pass through magnetic field lines with a mirror ratio of about 4 toward the region of analysis. In the discharge vessel, a Langmuir probe is installed for the measurement of temperature, density, and potential of the plasma adjacent to the region of analysis.

B. Omegatron

Figure 2 shows a schematic diagram of the omegatron with electronic circuits. The omegatron consists of a plasma end plate: (1) of 200 mm in diameter with an orifice of 1 mm in diameter, two 50×50 mm parallel plates [front plate (2) with the orifice and back plate (5)], two 100×50 mm parallel plates of a radio-frequency (rf) electrode (3) and ground electrode (4), and two 100×50 mm parallel side electrodes (7). All the plates are made of stainless steel of 1 mm thickness. Insulating materials are inserted in spaces along the plates to isolate each plate electrically. The plasma end plate, which is at a floating potential, divides the plasma production and analysis regions. Argon ions enter the region of analysis through a small floating aperture between the plasma end plate and the front plate on which a bias potential is applied. The control of the bias voltage has significant effects on the omegatron performance.[2–4] The dc bias voltage of the front plate is set to ~6 V. The back plate is also biased to ~6 V. The bias voltages produce electric fields which retard the ions with kinetic energy in the axial direction so that the rf electric field can accelerate the ions from rest. The employment of optimal biasing improves ion collection efficiency. The side plates are at the floating potential.

Five 18×5 mm ion collectors (6) placed on the ground electrode plate are used to measure ion currents. The clearance between the ion collectors themselves, and the front,

back, and ground electrode plates is 2 mm. An rf electric field is set up normal to the fixed magnetic flux density in the omegatron where the rf power (electric field $E_{\mathrm{rf}} \leqslant 200$ V/m in amplitude, excitation frequency $f_{\mathrm{rf}} < 20$ MHz) is supplied. When the applied frequency becomes close to the ion cyclotron frequency, the ions are expected to be accelerated and to increase their orbital radii and eventually strike the collector, indicating resonance behavior.[1] The ions flow into a collector and a time-averaged dc ion current is recorded with the X–Y recorder via a resistor. Thus, we can obtain a spectrum of the ion current as a function of rf excitation frequency.

C. Operation

The argon gas pressure p_{Ar}, magnetic flux density B, and rf voltage V_{rf}, vary in the ranges of $1.0\times10^{-4} \leqslant p_{\mathrm{Ar}} \leqslant 1.0\times10^{-3}$ Torr, $0.5 \leqslant B \leqslant 2.0$ T, and $1 \leqslant V_{\mathrm{rf}} \leqslant 10$ V, respectively. The peak value of ion current in the frequency spectrum I_{p} is defined as [intensity at ion cyclotron resonance frequency f_{ci}] − [intensity at the base of resonance peak]. The half width, Δf_{p} is defined as the full width of f_{rf} at the half maximum of ion current in the frequency spectrum. The mass resolution $m/\Delta m$ is defined as $f_{\mathrm{ci}}/\Delta f_p$.

The electron temperature and the electron density ($\cong$ion density) measured with the Langmuliar probe are 5.0 eV and of the order of 10^{15} m^{-3}, respectively, while the ion temperature is determined to be about 0.5 eV, from comparison with a measurement in another similar discharge experiment. These parameters have no significant dependence on the variations in the argon gas pressure and magnetic flux density in the region mentioned above.

III. NUMERICAL MODEL

In a number of previous studies, the mass resolution has been theoretically predicted without considering collisional effects in high-vacuum systems where ions strike the collector in the angular frequency range of $\Delta\omega = 2E_{\mathrm{rf}}/(R_0 B)$. Here, E_{rf} is the amplitude of rf electric field and R_0 is the length from the axis center to the collector.[1–3,5] In order to describe the ion behavior and the omegatron performance in a collision-dominated weakly ionized plasma under a high magnetic field, we adopt a simple numerical model employing the equation of single-particle motion, which takes into account the effects of ion collisions with neutral argon atoms.

A. Basic equation

The following assumptions are made. (a) The uniform magnetic flux density is temporally constant: $\mathbf{B} = (0,0,B_z)$ in an (x,y,z) coordinate. (b) A uniform rf electric field $\mathbf{E}_{\mathrm{rf}}(t) = (E_{\mathrm{rf}} \cos \omega_{\mathrm{rf}} t, 0, 0)$ is applied between the rf and ground electrode plates, where $\omega_{\mathrm{rf}} = 2\pi f_{\mathrm{rf}}$ is the excitation angular frequency. (c) The plasma consists of singly ionized argon atoms and electrons. The effects of collisions with argon neutral atoms are taken into account.

The following is a differential equation of the motion for the force exerted on an argon ion of charge e and velocity $\mathbf{v}_i$ by $\mathbf{E}_{\mathrm{rf}}(t)$, $\mathbf{B}$, and the quantity, $m_i \nu_i \mathbf{v}_i$, which represents the force experienced by the argon ion as a result of collisions with other particles

$$m_i \, d\mathbf{v}_i/dt = e\mathbf{v}_i \times \mathbf{B} + e\mathbf{E}_{\mathrm{rf}}(t) - m_i \nu_i \mathbf{v}_i, \tag{1}$$

where m_i, $\mathbf{v}_i$, and ν_i are mass, velocity, and collision frequency of the argon ions, respectively. On average, the effect of $m_i \nu_i \mathbf{v}_i$ is equivalent to drag on the argon ion, which may be approximated as the average rate at which momentum is lost in collisions. For the present collision-dominated weakly ionized argon plasma, the collision frequency is described as $\nu_i = \nu_{\mathrm{ion-neutral}} = n_{\mathrm{Ar}} Q_{\mathrm{Ar}} v_i$, where the momentum-transfer cross section between the argon ion and neutral species is assumed to be constant $Q_{\mathrm{Ar}} = \pi(2r_{\mathrm{Ar}})^2$ ($r_{\mathrm{Ar}} = 0.113$ nm).

Time-averaged ion velocity in the radial direction $\overline{U_r}$, which is a macroscopic consequence of cyclotron motions, is defined as

$$\overline{U_r} = \frac{1}{\tau}\int_0^{\tau} \frac{dr_i}{dt}\, dt, \tag{2}$$

where r_i is ion orbital radius and τ is characteristic time. The characteristic time τ is assumed to be the time required for ions to reach the collector at resonance, $\tau = 2BR_0/E_{\mathrm{rf}}$, given by the collisionless theory.[1] Time-averaged ion current density is written as

$$j = en_i \overline{U_r}. \tag{3}$$

This macroscopic current is considered to be a hypothetical current equivalent to the current of ions striking the collector in the real omegatron.

B. Calculation conditions

Initial conditions are as follows. In the experimental situation, the velocity distributions for ions, electrons, and neutral particles can be assumed to be Maxwellian with electron, ion, and neutral particle temperatures of $T_{\mathrm{e}} = 5.0$ eV, $T_i = 0.5$ eV, and $T_{\mathrm{Ar}} = 0.025$ eV, respectively. Since the equation of single-particle motion is applied in our model [see Eq. (1)], the initial ion velocity is determined to be $\mathbf{v}_{\mathrm{ini}} = (v_T, v_T, v_T)$, where $v_T = \sqrt{\kappa T_i/m_i}$ and κ is the Boltzmann constant. The initial ion position $(x_{\mathrm{ini}}, y_{\mathrm{ini}}, z_{\mathrm{ini}}) = (0,0,0)$ is the center of the orifice on the front plate. The equation of state for perfect gas $p_{\mathrm{Ar}} = n_{\mathrm{Ar}} \kappa T_{\mathrm{Ar}}$ is used. The argon ion density is constant $n_i = 3.0\times10^{15}$ m^{-3} corresponding to the experimental condition of argon gas pressure $p_{\mathrm{Ar}} = 3.0 \times 10^{-4}$ Torr.

The differential equation (1) is solved via a fourth-order Runge–Kutta method. The finest time step of less than 0.1 μs is used. The calculation time of about 1.0 ms is adequate for describing the resonance behavior. The calculated frequency resolution is less than 0.1 kHz.

IV. RESULTS AND DISCUSSION

A. Shape of ion current spectrum

In order to clarify the ion resonance behavior and the omegatron performance under the high-pressure condition, the frequency spectrum of ion current as a function of rf

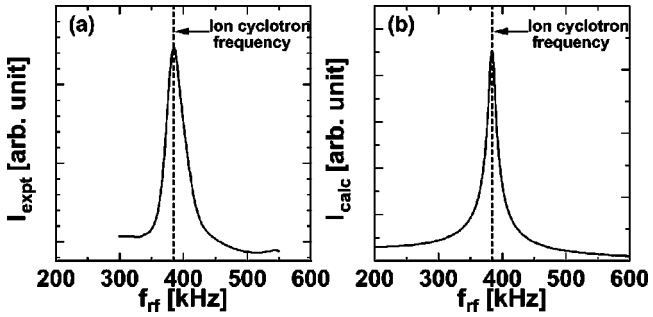

FIG. 3. (a) Measured ion current I_{expt} spectrum. (b) Calculated ion current I_{calc} spectrum. Conditions: argon gas pressure $p_{\mathrm{Ar}}=3.0\times10^{-4}$ Torr, magnetic flux density $B=1.0$ T, and rf voltage $V_{\mathrm{rf}}=10$ V.

voltage is experimentally examined and compared to the numerical calculations. Figures 3(a) and 3(b) show the shapes of the measured ion current I_{expt}, spectrum, and calculated ion current I_{calc} spectrum, respectively. Operation and calculation conditions are $p_{\mathrm{Ar}}=3.0\times10^{-4}$ Torr, magnetic flux density $B=1.0$ T, and rf voltage $V_{\mathrm{rf}}=10$ V. The ion-current spectral shape shown in Fig. 3(a) confirms that the analyzer's peak frequency is consistent with the ion cyclotron frequency of the argon ion $f_{\mathrm{ci}}=eB/2\pi m_i=384.5$ kHz. The calculated spectral shape shown in Fig. 3(b) agrees well with the measured result.

Figure 4(a) shows the measured peak ion current $I_{p,\mathrm{expt}}$ and calculated peak ion current $I_{p,\mathrm{calc}}$ as a function of V_{rf}. Since a large fraction of the ion current is measured by the middle collector (Fig. 2), the effective ion-collecting cross section is considered to be 0.9 cm^2. The ion current $I_{p,\mathrm{calc}}$ is estimated by multiplying the peak ion current density [Eq. (3)] by 0.9 cm^2. Figure 4(b) shows the V_{rf} dependence of measured and calculated mass resolution $m/\Delta m$. The theoretical mass resolution for the collisionless condition given by Sommer *et al.*[1] is also presented, where $m/\Delta m=eR_0B^2/2m_iE_{\mathrm{rf}}$. Calculation conditions are the same as the experimental ones. It is seen in Fig. 4(a) that the peak ion current increases with increasing V_{rf}. The V_{rf} dependence of the calculated ion current $I_{p,\mathrm{calc}}$ is consistent with the experimental result. On the other hand, the calculated ion current is higher than the measured ion current $I_{p,\mathrm{expt}}$, which implies

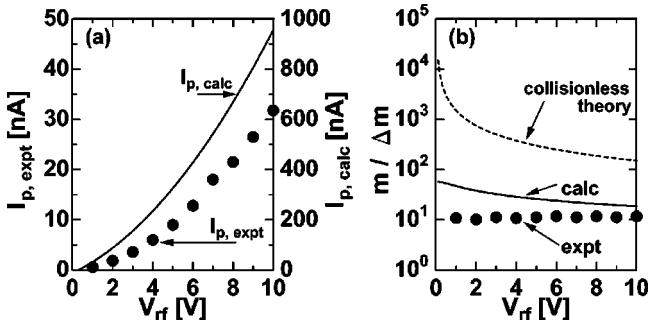

FIG. 4. (a) rf voltage V_{rf} dependence of measured peak ion current $I_{p,\mathrm{expt}}$ and calculated peak ion current $I_{p,\mathrm{calc}}$. (b) rf voltage V_{rf} dependence of measured and calculated mass resolution $m/\Delta m$. Calculation conditions: argon gas pressure $p_{\mathrm{Ar}}=3.0\times10^{-4}$ Torr and magnetic flux density $B=1.0$ T. Theoretical mass resolution given by the collisionless theory is plotted in (b).

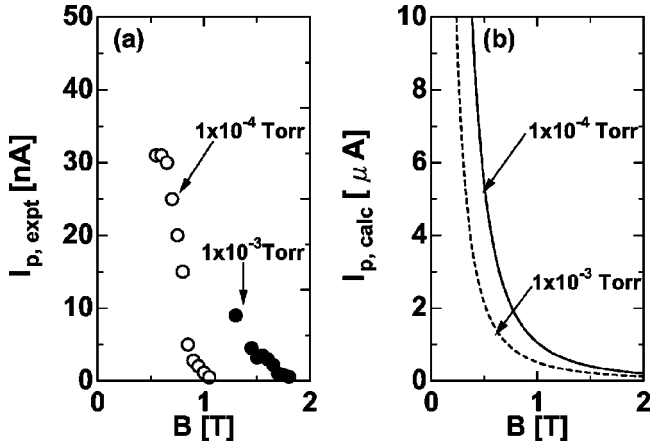

FIG. 5. (a) Measured magnetic flux density B dependence of peak ion current $I_{p,\mathrm{expt}}$ for typical pressures. Operation conditions: $p_{\mathrm{Ar}}=1.0\times10^{-4}$ and 1.0×10^{-3} Torr, $0.45\leqslant B\leqslant1.80$ T, and $V_{\mathrm{rf}}=10$ V. (b) Calculated magnetic flux density B dependence of peak ion current $I_{p,\mathrm{calc}}$ for typical pressures. Calculation conditions: $p_{\mathrm{Ar}}=1.0\times10^{-4}$ and 1.0×10^{-3} Torr, $B\leqslant2.0$ T, and $V_{\mathrm{rf}}=10$ V.

that there is room for further development of this calculation model for the estimation of net ion flux detected by the collector.

The collisionless theory[1] predicts that the half width Δm is proportional to rf voltage. Thus, the mass resolution derived from the collisionless theory deteriorates from 3.0×10^4 to 1.5×10^2 as V_{rf} is increased from 0.05 to 10 V, as indicated in Fig. 4(b). In contrast, the measured mass resolution $m/\Delta m_{\mathrm{expt}}$ is around 12 which is almost constant, being independent of V_{rf}. The calculated mass resolution $m/\Delta m_{\mathrm{calc}}$ decreases slightly from 58 to 19 with increasing V_{rf}. The spectral shape becomes broad under the present pressure condition due to collisional effects and the mass resolution is clearly degraded compared with the collisionless case. Since the increase in rf voltage enhances the ion current peak without any significant decrease in the mass resolution, as shown in the experimental results, the performance of mass spectroscopy is improved and the device functions well under such a high-gas-pressure condition.

B. Magnetic flux density and pressure dependence of mass resolution

The peak ion-current intensity and mass resolution as functions of magnetic flux density and argon gas pressure are discussed experimentally and numerically. Figure 5(a) shows the dependence of peak ion current $I_{p,\mathrm{expt}}$ on the measured magnetic flux density B for typical pressures $p_{\mathrm{Ar}}=1.0\times10^{-4}$ and 1.0×10^{-3} Torr, where V_{rf} and B are 10 V and 0.45–1.80 T, respectively. At $p_{\mathrm{Ar}}=1.0\times10^{-3}$ Torr, $I_{p,\mathrm{expt}}$ is not obtained under the condition of $B<1.30$ T because a stable plasma is not maintained when the magnetic flux density is insufficient in such a high-pressure region. Figure 5(b) shows the calculated dependence of peak ion current $I_{p,\mathrm{calc}}$, on the magnetic flux density B for typical pressures. The calculation conditions are $V_{\mathrm{rf}}=10$ V, $B\leqslant2.0$ T, and $p_{\mathrm{Ar}}=1.0\times10^{-4}$ and 1.0×10^{-3} Torr.

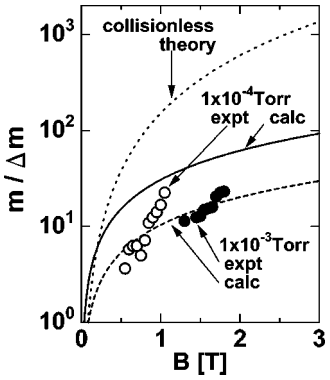

FIG. 6. Measured and calculated mass resolution $m/\Delta m$ as a function of magnetic flux density B for typical pressures. Mass resolution of the collisionless theory is also illustrated. Operation and calculation conditions are the same as those in the previous figures.

It is seen in Fig. 5(a) that $I_{p,\mathrm{expt}}$ decreases as magnetic flux density increases. The calculated result in Fig. 5(b) also shows that the ion current becomes lower at higher magnetic flux density. This tendency is independent of the pressure. The decrease in the ion current with increasing magnetic flux density is ascribed to an ion confinement effect by the applied magnetic flux density. Although the calculated ion current is higher than the measured one, the present numerical model well describes the magnetic flux density dependence of the ion current. Figure 5(b) shows that $I_{p,\mathrm{calc}}$ decreases with increasing pressure. This is not caused by the decrease in the ion density, which can be confirmed from the fact that the calculation is performed under the constant ion-density condition. The phenomenon is due to the decrease of ion velocity in the radial direction, which results from collision-frequency enhancement. The experimental result in Fig. 5(a) implies that $I_{p,\mathrm{expt}}$ at $p_{\mathrm{Ar}}=1.0\times10^{-3}$ Torr could be higher than that at 1.0×10^{-4} Torr under high magnetic flux density ($B>1$ T). A plausible explanation for this result is ascribed to the change in the experimental discharge situation, i.e., increase in the ion density at $p_{\mathrm{Ar}}=1.0\times10^{-3}$ Torr.

Figure 6 shows measured and calculated mass resolutions $m/\Delta m$ as a function of magnetic flux density B, where the mass resolution of the collisionless theory is illustrated; the conditions are the same as those in Fig. 5. The measured and calculated mass resolutions are lower than that of the collisionless theory. However, as the magnetic flux density increases from 0.05 to 1.05 and from 1.30 to 1.80 T, the measured mass resolution increases from 3.6 to 22.5 and from 11.4 to 23.1 at $p_{\mathrm{Ar}}=1.0\times10^{-4}$ and 1.0×10^{-3} Torr, respectively. The calculated mass resolution is improved following a trend comparable to the observed result when magnetic flux density is increased. Although the ion–neutral particle collisions deteriorate the mass resolution, the mass resolution is predominantly improved in proportion to the magnetic flux density. The collisional effect on the ion cyclotron resonance at the high pressure is clearly explained by the present numerical model. The result under the condition of $p_{\mathrm{Ar}}=1.0\times10^{-4}$ Torr shows that the measured mass resolution deviates from the calculated one at magnetic flux density less than 1.0 T. This is because nonresonant ions more strongly influence the mass resolution in the experiment than estimated by the calculation. In other words, the diffusion process of the nonresonant ions is not included in the calculation, while it becomes apparent, compared with the process of the exactly resonant ions in the experiment, when the magnetic flux density is insufficient.

Figures 5 and 6 indicate that reasonable mass spectra can be obtained with the mass resolution of more than 10 by applying a magnetic field of around 1.5 T even under the high-pressure condition on the order of 1.0×10^{-3} Torr.

V. SUMMARY

Direct mass spectrometry in the production region of the collision-dominated weakly ionized argon plasma has been demonstrated for the omegatron by employing the GM cryocooled superconducting magnet. A numerical model including collisional effects has been proposed to describe the performance of the omegatron.

The mass spectrometry has been successfully conducted using a high magnetic flux density of up to 2 T, even at a high pressure on the order of 10^{-3} Torr. The intensity of the ion-current peak, and mass resolution in the spectrum have been obtained experimentally and numerically as functions of pressure and magnetic flux density. Collisional effects on the omegatron performance were elucidated through a comparison of the experimental and calculated results. An increase of the rf voltage applied to the omegatron enhanced the ion spectrum intensity while the mass resolution remained almost constant, which resulted in the improvement of the omegatron performance. Although the mass resolution deteriorated under the high-pressure condition, it was predominantly improved in proportion to the magnetic flux-density intensity. The collisional effects and magnetic flux density dependence of the mass resolution at the high pressure were clearly explained by the present numerical model.

[1] H. Sommer, H. A. Thomas, and J. A. Hipple, Phys. Rev. **82**, 697 (1951).
[2] E. Y. Wang, L. Schmitz, Y. Ra, B. LaBombard, and R. W. Conn, Rev. Sci. Instrum. **61**, 2155 (1990).
[3] J. Friedmann, J. L. Shohet, and A. E. Wendt, IEEE Trans. Plasma Sci. **19**, 47 (1991).
[4] T. Hirata, R. Hatakeyama, Y. Yagi, T. Mieno, S. Iizuka, and N. Sato, J. Plasma Fusion Res. **71**, 615 (1995).
[5] T. Mieno, H. Kobayashi, and T. Shoji, Meas. Sci. Technol. **4**, 193 (1993).
[6] J. M. Dawson *et al.*, Phys. Rev. Lett. **37**, 1547 (1976).
[7] A. I. Karchevskii, V. S. Laz'ko, Yu. A. Muromkin, A. I. Myachkov, V. G. Pashkovskii, A. L. Ustinov, and A. V. Chepkasov, Plasma Phys. Rep. **19**, 214 (1993).
[8] A. Compant La Fontaine and V. G. Pashkovsky, Phys. Plasmas **2**, 4641 (1995).
[9] R. Hatakeyama, N. Y. Sato, and N. Sato, Nucl. Instrum. Methods Phys. Res. B **70**, 21 (1992).
[10] A. V. Timofeev, Plasma Phys. Rep. **25**, 207 (1999).
[11] B. J. Huang and S. C. Chang, Cryogenics **35**, 117 (1995).